GEOPHYSICAL RESEARCH LETTERS, VOL. 27, NO. 2, PAGES 181-184, JANUARY 15, 2000

The Formation of an Electron Hole in the Topside Equatorial Ionosphere

J.D. Huba and G. Joyce

Plasma Physics Division, Naval Research Laboratory, Washington, DC 20375

J.A. Fedder

Sachs-Freeman Associates, Landover, MD

Abstract. In this letter we report new modeling results that show the formation of an electron hole (depletion) in the topside equatorial ionosphere. The reduction in the electron density occurs in the altitude range 1500 - 2500 km at geomagnetic equatorial latitudes. The hole is produced by transhemispheric O^+ flows that collisionally couple to H^+ and transport it to lower altitudes, thereby reducing the electron density at high altitudes. The transhemispheric O^+ flows are caused by an interhemispheric pressure anisotropy that can be generated by the neutral wind, primarily during solstice conditions. The formation of the electron hole has a seasonal and longitudinal dependence. This result has been found with a new low-latitude ionospheric model that has been developed at the Naval Research Laboratory: SAMI2 (Sami2 is Another Model of the Ionosphere).

Introduction

Recently, a new low-latitude model of the ionosphere has been developed at the Naval Research Laboratory: SAMI2 (Sami2 is Another Model of the Ionosphere). SAMI2 treats the dynamic plasma and chemical evolution of seven ion species (H^+, He^+, N^+, O^+, N_2^+, NO^+, and O_2^+). The ion temperature equation is solved for three species: H^+, He^+, and O^+, as well as the electron temperature equation. The neutral species are specified using MSIS86 and HWM93. SAMI2 models the plasma along the earth's dipole field from hemisphere to hemisphere and includes the $\mathbf{E}\times\mathbf{B}$ drift of a flux tube (both in altitude and in longitude), as well as inertia in the ion momentum equation for plasma motion along the dipole field line. Existing ionospheric models [*Anderson et al.*, 1998; *Richards and Torr*, 1996; *Bailey and Balan*, 1996; *Anderson et al.*, 1996] assume the ions are collisional at all altitudes. To our knowledge, SAMI2 is the first low latitude ionospheric model to consider ion inertia.

In this letter we report the formation of a very high altitude electron depletion at equatorial latitudes. The electron hole occurs in the altitude range 1500 - 2500 km at geomagnetic equatorial latitudes. It is produced by transhemispheric O^+ flows that collisionally couple to H^+ and transport it to lower altitudes, and thereby reduce the electron density at high altitudes. The transhemispheric O^+ flows are caused by an interhemispheric pressure anisotropy that can be generated by the neutral wind, primarily during solstice conditions. The formation of the electron depletion has a seasonal and longitudinal dependence.

Paper number 1999GL010735.
00948276/99/1999GL010735$05.00

Basic Model and Equations

SAMI2 solves the plasma equations in an offset, tilted dipole frame of reference [*Bailey and Balan*, 1996]. The dipole coordinates are p, s, and ϕ where p denotes the L shell, s is along the field ($s = qr_E$ where q is the usual dipole coordinate and r_E is the radius of the earth), and ϕ is the longitudinal coordinate. For the purposes of this letter we will neglect motion in the ϕ direction. The magnetic field is in the $+s$ direction and is written as $\mathbf{B} = B_s\,\mathbf{e}_s$ where $B_s = B_0\left(1+3\cos^2\theta\right)^{1/2}\left(r_0/r\right)^3$.

The continuity, momentum, and temperature equations solved in SAMI2 are expressed as

$$\frac{\partial n_i}{\partial t} + \nabla\cdot(n_i\mathbf{V}_i) = \mathcal{P}_i - \mathcal{L}_i n_i \tag{1}$$

$$\frac{\partial \mathbf{V}_i}{\partial t} + \mathbf{V}_i\cdot\nabla\mathbf{V}_i = -\frac{1}{\rho_i}\nabla P_i + \frac{e}{m_i}\mathbf{E} + \frac{e}{m_i c}\mathbf{V}_i\times\mathbf{B} + \mathbf{g}$$
$$-\nu_{in}(\mathbf{V}_i - \mathbf{V}_n) - \sum_j \nu_{ij}\left(\mathbf{V}_i - \mathbf{V}_j\right) \tag{2}$$

$$0 = -\frac{1}{n_e m_e}\nabla P_e - \frac{e}{m_e}\mathbf{E} - \frac{e}{m_e c}\mathbf{V}_e\times\mathbf{B}\,. \tag{3}$$

$$\frac{\partial T_i}{\partial t} + \mathbf{V}_i\cdot\nabla T_i + \frac{2}{3}T_i\nabla\cdot\mathbf{V}_i + \frac{2}{3}\frac{1}{n_i k}\nabla\cdot Q_i = Q_{in} + Q_{ij} + Q_{ie} \tag{4}$$

$$\frac{\partial T_e}{\partial t} - \frac{2}{3}\frac{1}{n_e k}b_s^2\frac{\partial}{\partial s}\kappa_e\frac{\partial T_e}{\partial s} = Q_{en} + Q_{ei} + Q_{phe} \tag{5}$$

In the above, $\mathcal{P}_i$ is the ion production term (e.g., photoionization [*Strobel et al.*, 1974; *Richards et al.*, 1994], chemistry [*Bailey and Balan*, 1996; *Schunk and Sojka*, 1996], $\mathcal{L}_i$ is the ion loss term (e.g., chemistry, radiative recombination), Q_{in} is the ion-neutral heating rate, Q_{ie} is the ion-electron heating rate, Q_{ij} is the ion-ion heating rate, Q_{en} is the electron-neutral heating rate, Q_{ei} is the electron-ion heating rate, and Q_{phe} is the photoelectron heating rate. The heating terms are taken from Millward et al. (1996).

The ionospheric equations are solved along dipole field lines. A nonuniform grid is used similar to that described in Bailey and Balan (1996). The density, velocity, and temperature equations are treated as a system of advection/diffusion equations. The diffusion terms are backward biased for stability while the advection terms use an implicit donor cell method. This method does not linearize the equations or iterate the solutions, and therefore requires a smaller time step than fully implicit algorithms. A paper describing the details of the SAMI2 model (i.e., physics, chemistry,

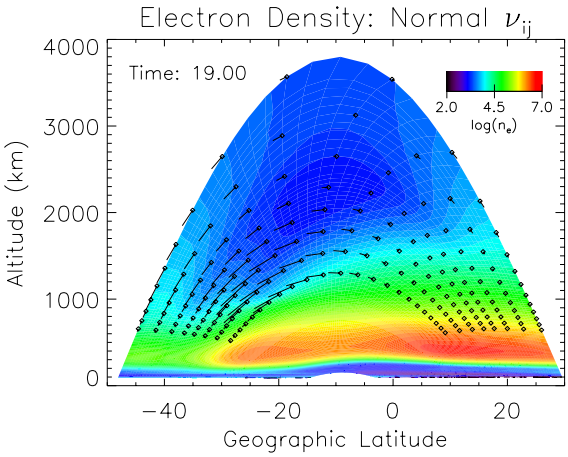

Figure 1. A color contour plot of the electron density as a function of geographic latitude and altitude at time $t = 1900$ LT. Also shown are the O^+ velocity vectors as 'wind flags'. The large dots lie on grid points and indicate the beginning of the velocity vector; the wind flags are plotted every fourth grid point above $\sim$ 600 km. The parameters used in this simulation are given in the text. Note the 'electron hole', closed dark blue contours, centered at $\sim$ 2100 km and $\theta_g \sim 15°$ S.

photoionization models, numerical algorithms, etc.) is in preparation.

Results

The simulation results presented use a mesh of 201 grid points for each flux tube and 96 flux tubes are modeled. The time step used is $\Delta t = 12$ s. The lower boundary of each flux tube is 90 km. The simulations are run for an initial 24 hrs to remove transients, and then run an additional 24 hrs to obtain diurnally converged results. A model zonal electric field is used that is proportional to $\sin[(t-7)/24]$ where t is the local time in hours. In general, the ionospheric flux tubes rise during the day from 0700 LT - 01900 LT, and fall during the night from 1900 LT - 0700 LT. The maximum vertical velocity is 20 m/s.

The first simulation results use the following parameters – day: 173 (summer solstice), longitude: 293.4 E (Arecibo), Ap: 2, F10.7: 180, and F10.7A: 180. Shown in Fig. 1 is a colored contour plot of the logarithm of the electron density as a function of geographic latitude versus altitude at time 1900 LT. Also shown are the O^+ velocity vectors which are denoted by 'wind flags'. The large dots lie on grid points and indicate the beginning of the velocity vector. The 'wind flags' are plotted every fourth grid point above $\sim$ 600 km. The maximum velocity shown is $\sim$ 400 m/s. The typical morphology of the ionosphere is observed in the results. During the day the ionosphere rises and the peak electron density reaches a few $\times 10^6$ cm^{-3} in the altitude range 250 - 400 km. During the night the ionosphere falls and the peak density drops to a few $\times 10^5$ cm^{-3} with a strong reduction in the electron density below 200 km. In Fig. 1 the Appleton anomaly is clearly evident. During the late afternoon and early evening (1600 LT - 2100 LT) the peak electron density occurs at the latitudes 25° S and 7° N in the altitude range 300 – 400 km. This latitudinal extent is roughly plus/minus 15 degrees from the magnetic equator. The most surprising result of this simulation is the formation of a hole (or depletion) in the topside electron density. The hole shows up as a closed, dark blue contour at $\sim$ 2000 km and $\theta_g \sim 15°$ S where the subscript g denotes the geographic coordinate system. It forms in the early afternoon and subsequently decays during the early morning hours. The hole is prominent in the altitude range 1500 - 2000 km and has a latitudinal extent of 20° S to 0° N for the ionospheric conditions modeled. It is localized about the geomagnetic equator, although for this longitude and season it is centered slightly south of the geomagnetic equator. These latitudinal ranges are for the longitude sector modeled, as there is also a longitudinal variation of the electron hole. Finally, we have run a high resolution case (401 grid points) and obtain similar results to those shown in Fig. 1.

In Fig. 2 we plot altitude profiles of the electron density for times $t =$ 0300 LT, 1200 LT, 1500 LT, and 1900 LT at a latitude of $\theta_g = 15°$ S. From the early morning hours ($\sim$ 0300 LT) until midday ($\sim$ 1200 LT) there is no high altitude electron hole. However, by the mid-afternoon ($\sim$ 1500 LT) the hole has clearly developed at an altitude $\sim$ 1900 km. There is a maximum in the electron density at $\sim$ 3000 km which can be interpreted as a new high altitude ionospheric layer. The electron density at $\sim$ 1900 km is a factor of $\sim$ 2 smaller than the secondary peak at $\sim$ 3000 km. The electron hole persists into the early evening and is evident at 1900 LT when it has risen in altitude to $\sim$ 2100 km. The hole eventually disappears in the early morning hours.

The physical mechanism for the topside electron depletion is as follows. The high altitude hole forms because transhemispheric oxygen ion flows collisionally pickup the hydrogen ions and transport them to lower altitudes. The resultant reduction of hydrogen ions at high altitudes over the geomagnetic equator is responsible for the electron depletion. In order for the hole to develop, relatively strong, persistent transhemispheric oxygen ion flows are necessary. These flows develop because of an asymmetric oxygen pressure profile along a magnetic flux tube. This asymmetric profile is more likely to form at the solstices because the

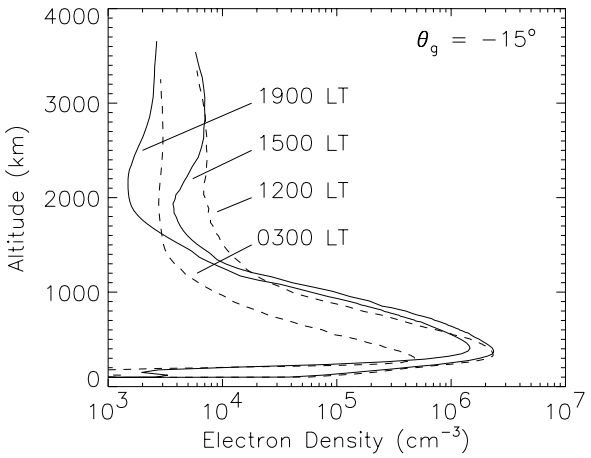

Figure 2. Plot of electron density versus altitude at for different times: 0300 LT, 1200 LT, 1500 LT, and 1900 LT. The geographic latitude is $\theta_g = 15°$ S. The electron hole is evident at times $t =$ 1500 LT and 1900 LT.

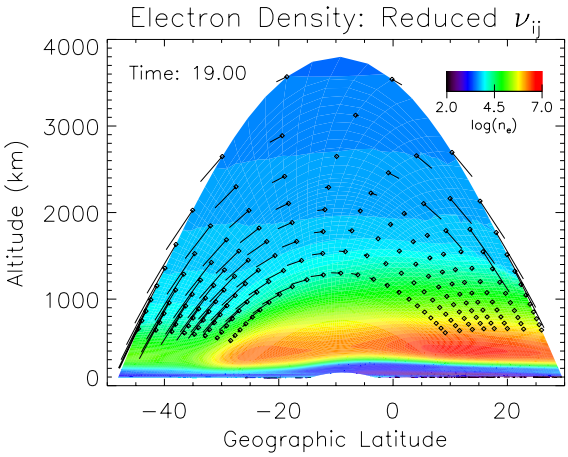

Figure 3. A color contour plot of the electron density as a function of geographic latitude and altitude. The parameters are the same as in Fig. 1 except that the ion-ion collision frequency has been reduced by a factor of 10. Note the absence of the electron hole and the larger O^+ velocities.

neutral wind transports oxygen ions to high altitudes on one side of the magnetic equator, and to low altitudes on the other side. In addition to transhemispheric O^+ flows, it is also required that the O^+ density be comparable to the H^+ density for efficient collisional coupling. The H^+/O^+ transition altitude over the geomagnetic equator ($\theta_g \simeq 9°$ S) is ~ 2500 km in the early afternoon when the hole forms; the transition altitude decreases to less the 1000 km prior to sunrise. However, the H^+/O^+ transition altitude over Arecibo ($\theta_g \simeq 18.5°$ N) is much lower at ~ 1500 km. This transition altitude is consistent with both observational and modeling results [*MacPherson et al.*, 1998]. We now present additional results which support our identification of the formation mechanism.

First, we show results of a simulation that uses the same parameters as Fig. 1 except that the ion-ion collision frequency has been arbitrarily reduced by a factor of 10. This reduces the collisional coupling between O^+ and H^+ and should have a significant impact on the formation of the electron hole if the above explanation is correct. The results are shown in Fig. 3 and, in fact, no electron hole is formed. Moreover, note that the O^+ velocities are larger than those shown in Fig. 1 because of the reduced drag by H^+.

Second, we show the results of a simulation for equinox conditions. The parameters used are the following: day 265 (fall equinox), longitude 23.4 E, Ap 2, F10.7 180, and F10.7A 180. This simulation shows that without a strong pressure anisotropy between the geomagnetic hemispheres there are no strong O^+ transhemispheric flows, and no electron hole should form. The results presented in Fig. 4 confirm this idea: no electron hole forms. The ionosphere is reasonably symmetric about the geomagnetic equator at $\sim 5°$, and the O^+ velocities are quite small compared to those in Figs. 1 and 3.

Finally, we have also run two other simulations for the parameters used in Fig. 1 in which the neutral wind and the zonal electric field were set to zero. For the case where $V_n = 0$, we find that no electron hole forms. This supports the interpretation that the neutral wind is the dominant mechanism to generate an interhemispheric O^+ pressure anisotropy that generates transhemispheric O^+ flows. For the case when $E_{zonal} = 0$, we find that an electron hole still forms, but at a later local time (~ 1700 LT). This suggests that the zonal electric field can affect the morphology of the electron hole but is not a causal mechanism.

Summary

We report the possible formation of a very high altitude electron hole in the equatorial ionosphere. It forms in the altitude range 1500 - 2500 km at geomagnetic equatorial latitudes. The hole is produced by transhemispheric O^+ flows that collisionally couple to H^+ and transport it to lower altitudes, thereby reducing the electron density at high altitudes. The transhemispheric O^+ flows are caused by an interhemispheric pressure anisotropy that can be generated by the neutral wind, primarily during solstice conditions. The formation of the electron hole has a seasonal and longitudinal dependence. This result has been found with a new low-latitude ionospheric model that has been developed at the Naval Research Laboratory: SAMI2 (Sami2 is Another Model of the Ionosphere). Animations of SAMI2 simulations can be found under the hyperlink 'Whatsnew' at *http://wwwppd.nrl.navy.mil*.

At this time we are not aware of experimental observations of a topside equatorial electron hole. The region in which the hole occurs – high altitude at equatorial latitudes – is difficult to diagnose; it is not accessible with ground-based radar and there is a dearth of *in situ* satellite measurements. Data which could possibly provide evidence of an electron hole is Alouette/ISIS topside sounder ionograms [*Benson*, 1996]. The satellites Alouette 2 and ISIS 1 had apogees of 3000 km and 3500 km, respectively, which are high enough to detect possible electron holes in the range 1500 – 2500 km. We are currently investigating the availability of suitable topside sounder data to search for the high altitude electron holes.

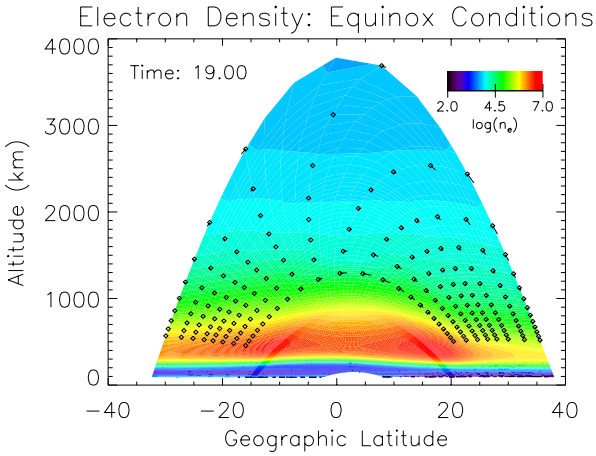

Figure 4. A color contour plot of the electron density as a function of geographic latitude and altitude for equinox conditions. The parameters used in this simulation are given in the text. The velocity vectors are much smaller than those in Figs. 1 and 3 and the electron hole is absent.

Acknowledgments. We thank P. Bernhardt, G. Bailey, and P. Richards for several helpful discussions during the development of SAMI2, and we thank R. Benson for discussions regarding topside sounder data. We also thank Ms. Sofia Herrero for assistance in developing the SAMI2 website. This research has been supported by the Office of Naval Research under the Advanced Research Initiative 'Ionospheric Specification and Forecasting.'

References

Anderson, D.N., D.T. Decker, and C.E. Valladares, Global Theoretical Ionospheric Model (GTIM), in *STEP: Handbook of Ionospheric Models*, ed. R.W. Schunk, 1996, p. 133.

Anderson, D.N., M.J. Buonsanto, M. Codrescu, D. Decker, C.G. Fesen, T.J. Fuller-Rowell, B.W. Reinisch, P.G. Richards, R.G. Roble, R.W. Schunk, and J.J. Sojka, Intercomparison of physical models and observations of the ionosphere, *J. Geophys. Res. 103*, 2179, 1998.

Bailey, G.J. and N. Balan, A Low-Latitude Ionosphere-Plasmasphere Model, in *STEP: Handbook of Ionospheric Models*, ed. R.W. Schunk, 1996, p. 173.

Benson, R.F., Ionospheric Investigations using Digital Alouette/ISIS Topside Sounder Ionograms, in *Proceedings of the* 1996 *Ionospheric Effects Symposium*, ed. J.M. Goodman, 1996, p. 202.

MacPherson, B., S.A. Gonzalez, G.J. Bailey, R.J. Moffett, and M.P. Sulzer, The effects of meridional neutral winds on the O^+-H^+ transition altitude over Arecibo, *J. Geophys. Res. 103*, 29,183, 1998.

Millward, G.H., R.J. Moffett, W. Quegan, and T.J. Fuller-Rowell, A Coupled Thermospheric-Ionospheric-Plasmasphere Model (CTIP), in *STEP: Handbook of Ionospheric Models*, ed. R.W. Schunk, 1996, p. 173.

Richards, P.G., J.A. Fennelly, and D.G. Torr, EUVAC: A Solar EUV Flux Model for Aeronomic Calculations, *J. Geophys. Res. 99*, 8981, 1994.

Richards, P.G. and D.G. Torr, The Field Line Interhemispheric Plasma Model, in *STEP: Handbook of Ionospheric Models*, ed. R.W. Schunk, 1996, p. 207.

Schunk, R.W. and J.J. Sojka, USU Model of the Global Ionosphere, in *STEP: Handbook of Ionospheric Models*, ed. R.W. Schunk, 1996, p. 153.

Strobel, D.F., T.R. Young, R.R. Meier, T.P. Coffey, and A.W. Ali, The Nighttime Ionosphere: *E* Region and Lower *F* Region, *J. Geophys. Res. 79*, 3171, 1974.

J.A. Fedder, J.D. Huba and G. Joyce, Code 6790, Naval Research Laboratory, Washington, DC 20375 (e-mail: huba@ppd.nrl.navy.mil)

(Received September 10, 1999; accepted October 19, 1999.)